JYX JYVÄSKYLÄN YLIOPISTO UNIVERSITY OF JYVÄSKYLÄ

This is a self-archived version of an original article. This version may differ from the original in pagination and typographic details.

Author(s): Morgan, Matthew M.; Nazari, Maryam; Pickl, Thomas; Rautiainen, J. Mikko; Tuononen, Heikki M.; Piers, Warren E.; Welch, Gregory C.; Gelfand, Benjamin S.

Title: Boron-nitrogen substituted dihydroindeno[1,2-b]fluorene derivatives as acceptors in organic solar cells

Year: 2019

Version: Accepted version (Final draft)

Copyright: © 2019 Royal Society of Chemistry

Rights: In Copyright

Rights url: http://rightsstatements.org/page/InC/1.0/?language=en

Please cite the original version:

Morgan, M. M., Nazari, M., Pickl, T., Rautiainen, J. M., Tuononen, H. M., Piers, W. E., Welch, G. C., & Gelfand, B. S. (2019). Boron-nitrogen substituted dihydroindeno[1,2-b]fluorene derivatives as acceptors in organic solar cells. Chemical Communications, 55(74), 11095-11098. https://doi.org/10.1039/C9CC05103A

COMMUNICATION

Boron-Nitrogen Substituted Dihydroindeno[1,2-*b*]fluorene Derivatives as Acceptors in Organic Solar Cells

Matthew M. Morgan,[a] Maryam Nazari,[a] Thomas Pickl,[a] J. Mikko Rautiainen,[b] Heikki M. Tuononen,[b] Warren E. Piers*,[a] Gregory C. Welch*,[a] and Benjamin S. Gelfand.[a]

The electrophilic borylation of 2,5-diarylpyrazines results in the formation of boron-nitrogen doped dihydroindeno[1,2-*b*]fluorene which can be synthesized using standard Schlenk techniques and worked up and handled readily under atmospheric conditions. Through transmetallation via diarylzinc reagents a series of derivatives were sythesized which show broad visible to near-IR light absorption profiles that highlight the versatility of this BN substituted core for use in optoelectronic devices. The synthesis is efficient, scalable and allows for tuning through changes in substituents on the planar heterocyclic core and at boron. Exploratory evaluation in organic solar cell devices as non-fullerene acceptors gave power conversion efficiencies of 2%.

Heteroatom doped polycyclic aromatic hydrocarbons (PAHs) are of interest in the field of organic materials because electronic properties can be manipulated while maintaining structural similarity. In this context, the substitution of C=C units with the isoelectronic and isosteric B-N subunit.[1-7] has been a fruitful strategy for providing novel extended π-materials,[8-10] including those for which the analogous all carbon frameworks are unavailable.[11] Accordingly, researchers have begun to use BN containing PAHs in organic light emitting diodes (OLEDs),[12] organic field effect transistors (OFETs)[7,12] and more recently in organic solar cells (OSCs).[13, 14]

OSCs are typically made using a blend of polymer or small molecule donors and acceptors, and matching optical, electronic, and packing properties are crucial to good device performance. To date there are far fewer electron accepting materials known, with fullerene-based acceptors being generally the most effective. More economically feasible, environmentally stable and easily tunable (in terms of optoelectronic and physical properties) acceptor materials are therefore desirable and this is where boron and BN doped conjugated molecules have seen the most promise. Most of the focus to date has been on well-studied BODIPY-based frameworks[15] or boron containing subpthalocyanines,[16-19] but more recently boron-nitrogen bipyridine derivatives[20, 21] have demonstrated high device performances.

To realize the potential of BN substituted frameworks as alternatives to fullerene acceptors there is a need for novel cores that are easy to synthesize on reasonable scales via methods that allow modular functionalization[22] in order to tune frontier orbital energies to match available donor species.

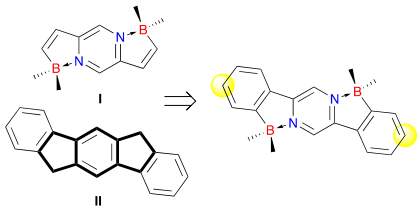

We have recently reported the 1,5-dibora-4a,8a-diaza indacene core[23] (**I**) and, based on the photophysical properties of these tricyclic derivatives, envisioned that the analogous BN doped version of the more π-extended pentacyclic dihydroindeno[1,2-*b*]fluorene framework **II** would have favourable acceptor properties for application in OSCs. The all carbon compounds have been studied extensively by Haley and co-workers in the context of conducting organic materials.[24] Here we report a convenient, scalable synthesis of a family BN-doped dihydroindeno[1,2-*b*]fluorenes that are air and water stable and exhibit tunable absorption properties depending on the nature of the substituents on either the B atom or the position marked in yellow on the flanking aryl rings. Furthermore, we demonstrate good initial OSC performance of one derivative when utilized as a non-fullerene acceptor paired with polymer-based donors.

The synthetic pathway to assemble the BN-dihydroindenylfluorenes, which engages established electrophilic borylation methodologies,[25-29] is summarized in Scheme 1 (See ESI for details). 2,5-Diarylpyrazines **1-Pz** and **2-Pz** (incorporating ^{t}Bu and N(4-^{t}BuPh)$_2$ groups in the R position, respectively) were prepared from 2,5-dibromopyrazine via

[a.] *Department of Chemistry, University of Calgary, 2500 University Drive N.W., Calgary, Alberta, T2N 1N4.*
[b.] *Department of Chemistry, Nanoscience Center, University of Jyväskylä, P.O. Box 35, FI-40014 Jyväskylä, Finland.*
Electronic Supplementary Information (ESI) available: Text and Figures giving further experimental and spectroscopic details, X-ray structural data for **1-Cl** and **1-FAr**, (CCDC 1937169-1937170) and full details on the computational results. See DOI: 10.1039/x0xx00000x

standard palladium catalysed cross coupling procedures[30] in good yields. Utilizing the electrophilic borylation conditions

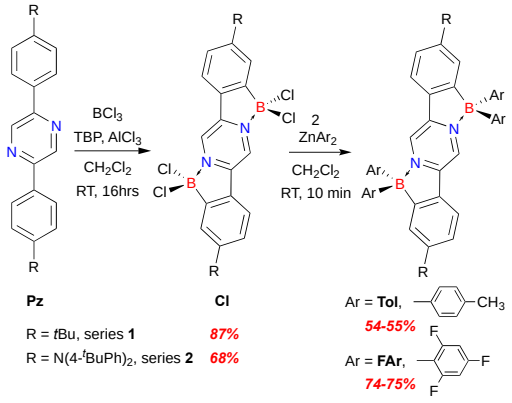

Scheme 1 Synthesis of compounds **1-Cl**, **2-Cl**, **1-Ar** and **2-Ar**.

reported by Ingelson *et al.* to prepare BN-fluorenes,[31] **1-Pz**/**2-Pz** were treated with BCl_3, $AlCl_3$ and the bulky base 2,4,6-tri-tertbutylpyridine (TBP) in dichloromethane to yield **1-Cl** and **2-Cl** in 87% and 68% yields respectively. These compounds were isolated in atmospheric conditions by washing the solids with water and hexanes and showed no decomposition due to hydrolysis of the B-Cl bonds. Substitution of the Cl ligands at boron with aryl groups was smoothly accomplished via treatment with 2 equivalents of a base-free diaryl zinc reagent, $ZnAr_2$ (Ar = tolyl,[32] 2,4,6-$F_3C_6H_2$[33]) to give the tetraarylated compounds **1-Tol**, **1-FAr**, **2-Tol** and **2-FAr** in moderate to good yields. The use of completely ether or THF-free $ZnAr_2$ reagents

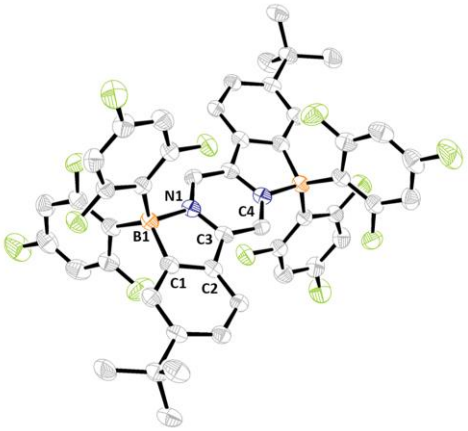

Figure 1. Molecular structure of **1-FAr**. Hydrogen atoms have been omitted for clarity. Thermal ellipsoids drawn at 50% probability level. Selected bond lengths (Å) B(1)-N(1) 1.642(6), B(1)-C(1) 1.618(6), C(1)-C(2) 1.404(6), C(2)-C(3) 1.453(6), C(3)-C(4) 1.398(6), N(1)-C(3) 1.348(6), N(1)-C(4) 1.327(5).

was critical to the success of these reactions. All six of these new BN-dihydroindenylfluorenes compounds were fully characterized and proved remarkably bench-stable with samples remaining spectroscopically pure even after several weeks under ambient conditions. The structures of **1-Cl** (Figure S1) and **1-FAr** (Figure 1) were confirmed through single crystal X-ray diffraction analysis. The structures indicate the pentacyclic core is perfectly planar, with B-N bond lengths of 1.615(6)Å (**1-Cl**) and 1.642(6) (**1-FAr**).

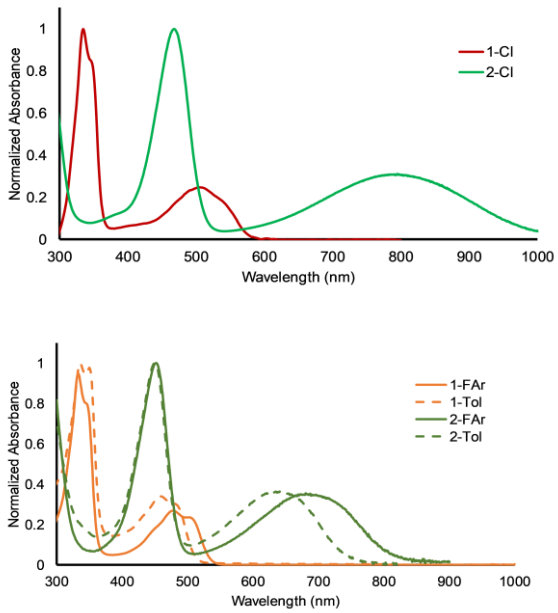

Figure 2 a) (top) Normalized absorption spectra in dichloromethane solutions of **1-Cl** and **2-Cl**. b) (bottom) Normalized absorption spectra in dichloromethane of arylated derivatives. For analogous plots of molar absorptivity vs wavelength, see ESI.

All six of the BN-doped dihydroindeno[1,2-*b*]fluorenes are all highly coloured and have broad absorption profiles with two major bands (Figure 2 and Table 1). TD-DFT (PBE0/Def-TZVP) analysis shows that these absorptions are associated with π- π^* transitions involving the planar pentacyclic core of the molecule; Figure 3 shows the frontier orbitals of **1-FAr** as a representative set, with details on the other compounds given in the ESI. The shorter wavelength absorption is primarily due to the HOMO-LUMO+1 transition and for the four compounds with electron withdrawing groups on B (*i.e.* Cl and FAr), the longer wavelength band (which exhibits some vibrational structure in the **1** series) is due to the HOMO-LUMO transition. For **1-Tol** and **2-Tol** (with more electron donating aryl groups on B), the HOMO is associated more with the π system of the tolyl groups and the π- π^* absorption observed involves HOMO-1 and HOMO-4 orbitals (Figure S2).

The position of these absorptions is strongly affected by the nature of the R group, with a significant red shift in both bands observed for the NAr_2 derivatives of the **2** series. The nature of the group on B does not dramatically affect the position of the high energy band, but does shift the lower energy absorption, particularly when substituting Cl for Ar. Compounds **1-Cl** and **1-FAr** are strongly emissive, exhibiting quantum yields of 0.63 and 0.85, respectively, and Stokes shifts of ≈ 2500 cm^{-1}. The localization of the LUMO on the pyrazine core gives this absorption some charge-transfer character that may enhance the emission Stokes shift. While we suspect the NAr_2 analogs **2-Cl** and **2-FAr** may also be emissive, we cannot detect this due to the low energies of the absorption bands. Interestingly, the tolyl-substituted derivative **1-Tol** is not emissive; this is likely due to the fundamentally different nature of the HOMO in this compound (Figure S2) as compared to **1-Cl** and **1-FAr**.

Table 1. Summary of photophysical, electrochemical, and OSC device data.

Comp	$\lambda_{abs,DCM}$ (ε) /nm ($10^4 M^{-1}cm^{-1}$)	λ_{Fl} (ϕ_f)[a] /nm(%)[b]	E_g^{opt} (eV)[c]	HOMO (eV)[d]	LUMO (eV)[d]	E_g^{elec} (eV)[d]	V_{oc} (V)[e]	J_{sc} (mA/cm^2)[e]	FF (%)[e]	PCE (%)[e]
1-FAr	332 (5.55) 482 (1.59)	547 (0.85)	2.27	-6.24	-3.88	2.36	0.87	5.4	40	1.9
2-FAr	451 (10.51) 670 (3.68)	--	1.48	-5.18	-3.66	1.52	0.79	1.2	31	0.3
1-Tol	338 (4.63) 462 (1.59)	not emissive	2.38	-6.01	-3.71	2.30	0.96	1.4	31	0.4
2-Tol	451 (6.93) 640 (2.54)	not emissive	1.64	-5.13	n/a	n/a	0.89	0.8	27	0.2
1-Cl	336 (4.01) 512 (1.01)	598 (0.63)	2.12	-6.41	-4.31	2.10	n/a	n/a	n/a	n/a
2-Cl	455 (7.49) 803 (2.26)	--	1.24	-5.22	-4.18	1.04	n/a	n/a	n/a	n/a

[a] Excited at 482 nm (**1-FAr**), 512 nm (**1-Cl**). [b] absolute quantum yield determined in CH_2Cl_2 solution using an integrating sphere. [c] calculated using the onset of absorption maxima. [d] $E_{LUMO} = -(4.8+E_{red})$, $E_{HOMO} = -(4.8+E_{ox})$.[e] All values based on OSC devices made from 1:1(Comp:PTB7-Th) weight ratio C_6H_5Cl solutions with a total solid concentration of 10 mg/mL (See ESI for further details).

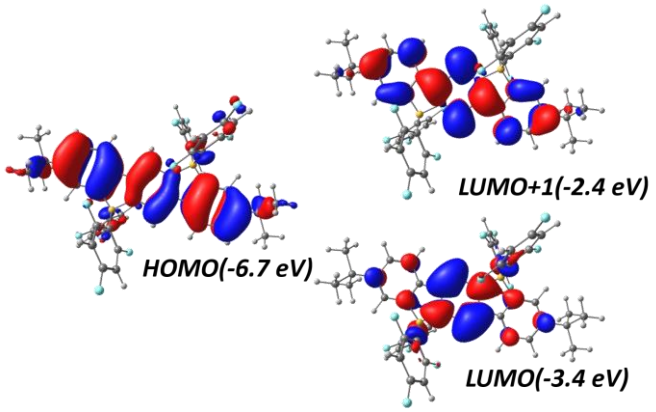

Figure 3 HOMO, LUMO and LUMO+1 orbitals of **1-FAr** based on calculations at the PBE0/Def-TZVP level.

The modification of the electronic structure across the series is further supported by the electrochemical data (Figures S3-10). The HOMO and LUMO energy levels of these molecules are estimated by cyclic voltammetry using the onset of both the reduction and oxidation peaks and are summarized in Table 1. Using **1-FAr** as an example, the estimated HOMO and LUMO energy levels are -6.41 eV and -4.31 eV, respectively, giving an electrochemical energy gap of 2.10 eV which matches closely with the photophysical gap of 2.12 eV. Across most of the series the optical and electrochemical band gaps are in good agreement, except **2-Cl** where the values differ by 0.20 eV, and **2-Tol** where the electrochemical reduction peak could not be observed. This lack of a reduction wave could be due to the low solubility of **2-Tol** as even for **2-FAr** which shows higher solubility, the oxidative couple is significantly smaller in magnitude than the reduction (Figures S9-10).

The broad absorption profiles and the favorable frontier orbital energies led us to explore the use of this family of BN-dihydroindenylfluorenes as non-fullerene acceptors[34, 35] in OSC devices. Proof-of-concept OSC devices were first fabricated using the compound **1-FAr** and three common high-performance donor polymers, namely PTB7-Th, PBDB-T, and PPDT2FBT (see Figure S11 for chemical structures). Although all compounds were subjected to preliminary testing, **1-FAr** was selected for detailed studies since it has the deepest electronic energy levels (Figure S12) and strong visible absorption, both complementary to the low-band gap donor polymers. OSC devices were constructed using the inverted architecture with active layers processed from C_6H_5Cl in air (Full details are found in the supporting information). The three active layers PTB7-Th:**1-FAr**, PBDB-T:**1-FAr**, and PPDT2FBT:**1-FAr** resulted in working devices with photodiode behaviour (Table 1 and Figure S11). In all cases panchromatic optical absorption and polymer emission quenching was observed (Figure S13). Device metrics are summarized in Table S1. The best OSCs were those based on PTB7-Th:**1-FAr** active layer with an open-circuit voltage of 0.89V, a short-circuit current of 5.6 mA cm^2 and a fill factor of 40% giving a respectable initial power conversion efficiency (PCE) of 2% (average PCE of 1.5% over 10 measurements). OSCs based on the PBDB-T:**1-FAr** and PPDT2FBT:**1-FAr** active layers had PCEs of 1%, owing to lower photocurrent generation. An examination of the active layer surface using atomic force microscopy revealed highly uniform and very smooth surfaces (Figure S14). This, coupled with a low shunt resistance implies minimal phase separation, thus we targeted the higher performing PTB7-Th:**1-FAr** system for further optimization. Unfortunately changing the donor:acceptor ratio or using volatile solvent processing additives did not improve the OSC device PCE (Table S2). Screening of the other materials **1-Tol**, **2-Tol**, and **2-FAr** using PTB7-Th gave OSCs with inferior perforce (ca. PCE 0.2-0.4%) when compared to the OSCs using the **1-FAr** based blends (Table S3), thus identifying the **1-FAr** as the target compound to structurally evolve into a new family of non-fullerene acceptors.

In conclusion, electrophilic borylation was utilized to synthesize a new family of air and moisture stable B-N doped π–conjugated organic molecules with promising properties for application as electron acceptors. Organic solar cells using **1-FAr** as the acceptor molecule led to devices with power conversion efficiencies of 2%. While device performance is low, the good open-circuit voltages (*ca.* > 0.8V) and uniform film formation make this system attractive for targeted acceptor synthesis. Indeed, the R groups employed (tBu and NAr_2) are far from ideal and use of planar electronic deficient capping units[20, 36-38] offer a clear direction for further research aimed at performance optimization of this class of acceptors in OSC devices.

Funding for this work was provided by NSERC of Canada in the form of a Discovery Grant to W.E.P. and the U of Jyväskylä and Emil Aaltonen Foundation to H. M. T. W.E.P. and G. C. W. acknowledge the Canada Research Chair secretariat for a Tier I CRC (2013–2020). and a Tier II Chair, respectively. M. M. M. thanks NSERC of Canada for PGSD Scholarship support. M. N. thanks the U Calgary for an Eyes High Scholarship.

Conflicts of interest

There are no conflicts to declare.

Notes and references

1. Z. Liu and T. B. Marder, *Angew. Chem. Int. Ed.*, 2008, **47**, 242-244.
2. M. J. D. Bosdet and W. E. Piers, *Can. J. Chem.*, 2009, **87**, 8-29.
3. F. Jäkle, *Chem. Rev.*, 2010, **110**, 3985-4022.
4. X.-Y. Wang, J.-Y. Wang and J. Pei, *Chem. Eur. J.*, 2015, **21**, 3528-3539.
5. J. Huang and Y. Li, *Front. Chem.*, 2018, **6**, 1-22.
6. Z. X. Giustra and S.-Y. Liu, *J. Am. Chem. Soc.*, 2018, **140**, 1184-1194.
7. P. G. Campbell, A. J. V. Marwitz and S.-Y. Liu, *Angew. Chem. Int. Ed.*, 2012, **51**, 6074-6092.
8. T. Hatakeyama, S. Hashimoto, S. Seki and M. Nakamura, *J. Am. Chem. Soc.*, 2011, **133**, 18614-18617.
9. X.-Y. Wang, F.-D. Zhuang, R.-B. Wang, X.-C. Wang, X.-Y. Cao, J.-Y. Wang and J. Pei, *J. Am. Chem. Soc.*, 2014, **136**, 3764-3767.
10. X.-Y. Wang, A. Narita, X. Feng and K. Müllen, *J. Am. Chem. Soc.*, 2015, **137**, 7668-7671.
11. B. Neue, J. F. Araneda, W. E. Piers and M. Parvez, *Angew. Chem. Int. Ed.*, 2013, **52**, 9966-9969.
12. D. Li, H. Zhang and Y. Wang, *Chem. Soc. Rev.*, 2013, **42**, 8416-8433.
13. S. Shimizu, T. Iino, A. Saeki, S. Seki and N. Kobayashi, *Chem. Eur. J.*, 2015, **21**, 2893-2904.
14. Y. Kubo, D. Eguchi, A. Matsumoto, R. Nishiyabu, H. Yakushiji, K. Shigaki and M. Kaneko, *J. Mater. Chem. A*, 2014, **2**, 5204-5211.
15. A. M. Poe, A. M. Della Pelle, A. V. Subrahmanyam, W. White, G. Wantz and S. Thayumanavan, *Chem. Commun.* 2014, **50**, 2913-2915.
16. K. Cnops, B. P. Rand, D. Cheyns, B. Verreet, M. A. Empl and P. Heremans, *Nat. Commun.*, 2014, **5**, 1-6.
17. C. Duan, G. Zango, M. García Iglesias, F. J. M. Colberts, M. M. Wienk, M. V. Martínez-Díaz, R. A. J. Janssen and T. Torres, *Angew. Chem. Int. Ed.*, 2017, **56**, 148-152.
18. B. Ebenhoch, N. B. A. Prasetya, V. M. Rotello, G. Cooke and I. D. W. Samuel, *J. Mater. Chem. A*, 2015, **3**, 7345-7352.
19. G. E. Morse and T. P. Bender, *ACS Appl. Mater. Interfaces*, 2012, **4**, 5055-5068.
20. F. Liu, Z. Ding, J. Liu and L. Wang, *Chem. Commun.*, 2017, **53**, 12213-12216.
21. T. Wang, C. Dou, J. Liu and L. Wang, *Chem. Eur. J.*, 2018, **24**, 13043-13048.
22. M. M. Morgan and W. E. Piers, *Dalton Trans.*, 2016, **45**, 5920-5924.
23. M. M. Morgan, E. A. Patrick, J. M. Rautiainen, D. M. Spasyuk, H. M. Tuononen and W. E. Piers, *Organometallics*, 2017, **36**, 2541-2551.
24. C. K. Frederickson, B. D. Rose and M. M. Haley, *Acc. Chem. Res.*, 2017, **50**, 977-987.
25. M. J. S. Dewar and R. Dietz, *J. Chem. Soc.*, 1959, 2728-2730.
26. N. Ishida, T. Moriya, T. Goya and M. Murakami, *J. Org. Chem.*, 2010, **75**, 8709-8712.
27. D. L. Crossley, I. A. Cade, E. R. Clark, A. Escande, M. J. Humphries, S. M. King, I. Vitorica-Yrezabal, M. J. Ingleson and M. L. Turner, *Chem. Sci.*, 2015, **6**, 5144-5151.
28. C. Z. Zhu, Z. H. Guo, A. U. Mu, Y. Liu, S. E. Wheeler and L. Fang, *J. Org. Chem.*, 2016, **81**, 4347-4352.
29. Y. C. Li, H. F. Meng, D. Yan, Y. Q. Li, B. Pang, K. Zhang, G. G. Luo, J. H. Huang and C. L. Zhan, *Tetrahedron*, 2018, **74**, 4308-4314.
30. S. Culham, P. H. Lanoë, V. L. Whittle, M. C. Durrant, J. A. G. Williams and V. N. Kozhevnikov, *Inorg. Chem.*, 2013, **52**, 10992-11003.
31. D. L. Crossley, J. Cid, L. D. Curless, M. L. Turner and M. J. Ingleson, *Organometallics*, 2015, **34**, 5767-5774.
32. J. J. Dunsford, E. R. Clark and M. J. Ingleson, *Angew. Chem. Int. Ed.*, 2015, **54**, 5688-5692.
33. Y. F. Al-Khafaji, M. R. J. Elsegood, J. W. A. Frese and C. Redshaw, *RSC Adv.*, 2017, **7**, 4510-4517.
34. C. Q. Yan, S. Barlow, Z. H. Wang, H. Yan, A. K. Y. Jen, S. R. Marder and X. W. Zhan, *Nat. Rev. Mater.*, 2018, **3**.
35. J. H. Hou, O. Inganas, R. H. Friend and F. Gao, *Nat. Mater.*, 2018, **17**, 119-128.
36. S. Holliday, R. S. Ashraf, A. Wadsworth, D. Baran, S. A. Yousaf, C. B. Nielsen, C. H. Tan, S. D. Dimitrov, Z. R. Shang, N. Gasparini, M. Alamoudi, F. Laquai, C. J. Brabec, A. Salleo, J. R. Durrant and I. McCulloch, *Nat. Commun.*, 2016, **7**.
37. J. Yuan, T. Y. Huang, P. Cheng, Y. P. Zou, H. T. Zhang, J. L. Yang, S. Y. Chang, Z. Z. Zhang, W. C. Huang, R. Wang, D. Meng, F. Gao and Y. Yang, *Nat. Commun.*, 2019, **10**.
38. Y. Cui, H. F. Yao, J. Q. Zhang, T. Zhang, Y. M. Wang, L. Hong, K. H. Xian, B. W. Xu, S. Q. Zhang, J. Peng, Z. X. Wei, F. Gao and J. H. Hou, *Nat. Commun.*, 2019, **10**.